

Online Research @ Cardiff

This is an Open Access document downloaded from ORCA, Cardiff University's institutional repository: <http://orca.cf.ac.uk/122622/>

This is the author's version of a work that was submitted to / accepted for publication.

Citation for final published version:

Lui, K. H., Jones, Tim, Berube, Kelly, Sai Hang Ho, Steven, Yim, S. H. L, Cao, Jun-Ji, Lee, S. C., Tian, Linwei, Wi Min, Dae and Ho, K. F. 2019. The effects of particle-induced oxidative damage from exposure to airborne fine particulate matter components in the vicinity of landfill sites on Hong Kong. *Chemosphere* 230 , pp. 578-586. 10.1016/j.chemosphere.2019.05.079 filefilefile

Publishers page: <https://doi.org/10.1016/j.chemosphere.2019.05.079>
<<https://doi.org/10.1016/j.chemosphere.2019.05.079>>

Please note:

Changes made as a result of publishing processes such as copy-editing, formatting and page numbers may not be reflected in this version. For the definitive version of this publication, please refer to the published source. You are advised to consult the publisher's version if you wish to cite this paper.

This version is being made available in accordance with publisher policies. See <http://orca.cf.ac.uk/policies.html> for usage policies. Copyright and moral rights for publications made available in ORCA are retained by the copyright holders.



1 **The effects of particle-induced oxidative damage from exposure to airborne fine**
2 **particulate matter components in the vicinity of landfill sites on Hong Kong**

3 K. H. Lui^{1,10}, Tim P. Jones², Kelly BéruBé³, Steven Sai Hang Ho⁴, S.H.L. Yim^{5,6}, Jun-Ji
4 Cao^{4,7}, S. C. Lee⁸, Linwei Tian⁹, Dae Wi Min¹⁰, K. F. Ho^{1*}

5
6 ¹ *The Jockey Club School of Public Health and Primary Care, The Chinese University of Hong*
7 *Kong, Hong Kong, China*

8 ² *School of Earth and Ocean Sciences, Cardiff University, Park Place, Cardiff, U.K.*

9 ³ *School of Biosciences, Cardiff University, Museum Avenue, Cardiff, U.K.*

10 ⁴ *Key Division of Atmospheric Sciences, Desert Research Institute, Reno, NV 89512, U.S.A.*

11 ⁵ *Department of Geography and Resource Management, The Chinese University of Hong*
12 *Kong, Hong Kong, China*

13 ⁶ *Stanley Ho Big Data Decision Analytics Research Centre, The Chinese University of Hong*
14 *Kong, Shatin, N.T., Hong Kong, China*

15 ⁷ *Institute of Global Environmental Change, Xi'an Jiaotong University, Xi'an, China*

16 ⁸ *Department of Civil and Structural Engineering, Research Center of Urban Environmental*
17 *Technology and Management, The Hong Kong Polytechnic University, Hong Kong, China*

18 ⁹ *School of Public Health, The University of Hong Kong, Hong Kong, China*

19 ¹⁰ *Division of Environmental Science and Engineering, Pohang University of Science and*
20 *Technology (POSTECH), Pohang 37673, Korea*

21
22
23 *Corresponding author. Tel.: +852 22528763; fax: +852 26063500

24 E-mail address: kfho@cuhk.edu.hk

25

26

27 **Abstract**

28 The physical, chemical and bioreactivity characteristics of fine particulate matter (PM_{2.5})
29 collected near (< 1km) two landfill sites and downwind urban sites were investigated. The
30 PM_{2.5} concentrations were significantly higher in winter than summer. Diurnal variations of
31 PM_{2.5} were recorded at both landfill sites. Soot aggregate particles were identified near the
32 landfill sites, which indicated that combustion pollution due to landfill activities was a
33 significant source. High correlation coefficients (*r*) implied several inorganic elements and
34 water-soluble inorganic ions (vanadium (V), copper (Cu), chloride (Cl⁻), nitrate (NO₃⁻), sodium
35 (Na) and potassium (K)) were positively associated with wind flow from the landfill sites.
36 Nevertheless, no significant correlations were also identified between these components
37 against DNA damage. Significant associations were observed between DNA damage and some
38 heavy metals such as cadmium (Cd) and lead (Pb), and total Polycyclic Aromatic
39 Hydrocarbons (PAHs) during the summer. The insignificant associations of DNA damage
40 under increased wind frequency from landfills suggested that the PM_{2.5} loading from sources
41 such as regional sources was possibly an important contributing factor for DNA damage. This
42 outcome warrants the further development of effective and source-specific landfill
43 management regulations for particulate matter production control to the city.

44

45

46

47

48

49 ***Keywords:***

50 Landfills; PM_{2.5}; Ambient air; Landfill composites; Oxidative potential

51

52 1. Introduction

53 Landfill has been traditionally regarded as a common method of organized waste disposal and
54 is a widely used waste management practice around the world. According to the Hong Kong
55 Environmental Protection Department, the disposal of total solid waste at landfills averages
56 15,102 tonnes per day, with 10,159 tonnes per day classified as municipal solid waste (MSW)
57 (e.g. domestic waste, commercial waste and industrial waste). The average disposal rate of
58 MSW in Hong Kong was approximately 1.4 kg per capita daily (HKEPD, 2015), compared to
59 approximately 2.0 kg per capita daily in the United States (U.S. EPA, 2013). The problem of
60 waste disposal is considered as one of the most serious environmental issues in Hong Kong.
61 Operating landfills can generate a variety of air pollutants such as particulate matter (PM) and
62 the emitted particulates can contain inorganic and organic components (Koshy et al., 2009;
63 Macklin et al., 2011). A study by Deed (2004) showed a large proportion of the inorganic
64 components in PM collected at landfills are mineral-based and derived from wind-blown soil.
65 Typical hazardous particles generated at landfills are toxic crystalline silica and needle-like
66 metal particles that are generated by waste fragmentisers.

67 Airborne PM is a health concern worldwide due to adverse health effects. A previous
68 epidemiological study demonstrated exposure to PM could intensify respiratory morbidity and
69 mortality (Pope III et al., 1995). Oxidative stress is a mechanism by which exposure to PM can
70 potentially cause adverse health effects when overproduction of oxidants (e.g., Reactive
71 Oxygen Species (ROS) and free radicals) offsets anti-oxidative defences (Charrier et al., 2014).
72 Fine particulate matter (aerodynamic diameter $< 2.5 \mu\text{m}$: $\text{PM}_{2.5}$) can elicit adverse
73 inflammatory responses by depositing in the lung periphery (Bitterle et al., 2006). The plasmid
74 scission assay (PSA) is an established technique for assessing the oxidative capacity (ROS)
75 (Gilmour et al., 1994; Stone et al., 1998; Moreno et al., 2004; Lingard et al., 2005; Miller et
76 al., 2012). Previous studies have applied this technique to understand the toxicity of

77 atmospheric particulates (Koshy et al., 2007; Koshy et al., 2009; Shao et al., 2013; Xiao et al.,
78 2014). The components such as elemental carbon (EC) and organic carbon (OC) can constitute
79 a significant proportion of PM_{2.5} (20-80%) (Rogge et al., 1993; Sillanpää et al., 2005). The
80 water-soluble fractions of atmospheric aerosol contains components (e.g. ions) that capable to
81 increase the solubility of toxic organic compounds (e.g. polycyclic aromatic hydrocarbons:
82 PAHs) and further to increase toxicity to human health (Wang et al., 2003). The bioavailable
83 transition metals on the particle surfaces can also promote free radicals generation and lead to
84 oxidative damage (Costa and Dreher, 1997; Donaldson et al., 1996).

85 Several studies have revealed the health risks posed by landfill sites (such as cancer or
86 congenital anomalies) (Jarup et al., 2012; Palmer et al., 2005), but there is insufficient
87 investigations about the bioactivity of PM_{2.5} from municipal landfill sites in Hong Kong. The
88 aims of this study are to: 1) To investigate the physicochemical characteristics of PM_{2.5} samples
89 collected from locations near (< 1km) MSW landfill sites; 2) To determine the oxidative stress
90 of PM_{2.5} samples using the generation of reactive oxygen species (ROS); 3) To determine the
91 relationship between physical and chemical characteristics of PM_{2.5} and their bioreactivity
92 collected near (< 1km) the landfill sites and in the downwind urban sites.

93

94 **2. Materials and methods**

95 2.1 Sampling locations

96 Five sampling sites were selected for this study (Figure 1). Two sites were located adjacent to
97 the landfill areas (with both <500 m from the landfill sites) namely West New Territories
98 (WENT) and South East New Territories (SENT). The WENT landfill has an area of 110 ha
99 with waste intake ~ 7,500 tonnes per day (HKEPD, 2015). The sampling site of WENT was
100 located at Ha Pak Nai, which was 100 m away from the WENT landfill. The SENT landfill has

101 an area of 100 ha waste intake ~4,000 tonnes per day (HKEPD, 2015). The sampling site of
102 SENT was located at Tseung Kwan O Industrial Estate approximately 300 m from the SENT
103 landfill. Two urban sites were located in a mixture of residential and commercial areas namely
104 as Tin Shui Wai (TSW) and Tseung Kwan O (TKO), which are the nearest local hubs to WENT
105 and SENT landfill respectively. The SENT landfill was to receive only construction waste after
106 January of 2016 to address the odour problem. The waste intake at the SENT Landfill was
107 anticipated to be reduced to approximately 500 vehicular loads after the regulation amendment
108 (HKEPD, 2016). Hok Tsui (HT) was selected as the rural site at the south-eastern tip of Hong
109 Kong Island. The sampling site is in a remote area and far removed from any anthropogenic
110 activities, ~2.5 km away from major traffic (Shek O Road). Details of sampling sites can be
111 found in Figure S1-2 (Supplementary Material).

112

113 2.2 Experimental procedures

114 2.2.1 Sample collection

115 Details of the sample collection can be found in Text S1 (Supplementary Material).

116

117 2.3 Analytical methods

118 2.3.1 Field emission scanning electron microscope (FESEM) analysis

119 The FESEM analysis was used for particle imaging according to standard procedures (Jones et
120 al., 2006). Particles on the Teflon filters were extracted with distilled deionized water, as this
121 extractant was considered to be least chemically aggressive solution. This extraction was
122 essential as the particles were embedded deep in the body of the filters and not seen on the
123 filter surface. A consequence of this is that all water-soluble samples are lost in these analyses.
124 The samples were then mounted on a conventional 12.5 mm aluminium stubs using Epoxy
125 resin (Araldite™). Stubs were coated to improve imaging with evaporated gold–palladium

126 (Au–Pd 60: 40), using a Bio-Rad SC500 sputter coater under an inert argon atmosphere, to a
127 thickness of 20 nm. A Veeco FEI Philips XL30 environmental SEM with a field emission gun
128 was used for specimen imaging.

129

130 2.3.2 Chemical components analysis

131 Details of the chemical components (elements, water-soluble inorganic ions, organic carbon,
132 elemental carbon and polycyclic aromatic hydrocarbons) analysis can be found in Text S2-5
133 (Supplementary Material). The abbreviation of individual chemical components can be
134 referred to Table S2 (Supplementary Material).

135

136 2.3.3 Plasmid scission assay (PSA) for bioreactivity analysis

137 Details of the plasmid scission assay analysis can be found in Text S6 (Supplementary
138 Material).

139

140 2.4 Statistical analysis

141 Statistical analysis was performed using SPSS 21.0 software. Details of the analysis can be
142 found in Text S7. The significance level was set at $p < 0.05$.

143

144 3. Results and discussion

145 3.1 Diurnal variations of PM_{2.5}

146 The PM_{2.5} mass concentrations acquired from real-time monitors have been cross-checked with
147 filter-based concentration results to ensure performance optimization. Good correlations were
148 observed between filter-based PM_{2.5} mass concentrations and real time PM_{2.5} mass
149 concentrations at WENT and SENT in both seasons (Winter season: WENT: $r = 0.88$, $p < 0.01$,
150 SENT: $r = 0.705$, $p < 0.01$; Summer season: WENT: $r = 0.89$, $p < 0.01$, SENT $r = 0.90$, $p <$

151 0.01). Figures 2 and 3 show temporal variations of hourly $PM_{2.5}$ level at WENT and SENT in
152 winter and summer, respectively. Diurnal variations of $PM_{2.5}$ (Supplementary Materials: Figure
153 S10) were observed in both landfill sites (especially in WENT). Pronounced diurnal variations
154 of $PM_{2.5}$ concentrations were observed for WENT in both seasons. In WENT, $PM_{2.5}$
155 concentrations in winter were generally low from December to January, followed by reaching
156 optimum in February. In summer, $PM_{2.5}$ concentrations were in general low from August to
157 September and achieved maximum in early October. The $PM_{2.5}$ concentrations were
158 subsequently decreased until November. In SENT, $PM_{2.5}$ concentrations reached minimum in
159 January and increased in February. In summer, $PM_{2.5}$ concentrations were at minimum from
160 July to August, followed by a peak observed in October. In addition, the $PM_{2.5}$ concentrations
161 were significantly higher in winter than summer. In WENT high $PM_{2.5}$ levels were due to
162 enhanced anthropogenic emissions with daytime activities (including landfill activities) in
163 addition to local land–sea breeze circulations. In SENT high $PM_{2.5}$ levels were also observed
164 during daytime, but the PM diurnal variations were different between seasons.

165 The contribution of $PM_{2.5}$ from different wind directions is illustrated by pollution roses in
166 Figure S6 (Supplementary Material). The dominant wind directions at WENT was south/north
167 in winter and south in summer. The $PM_{2.5}$ loadings were observed to increase under the
168 dominant west and northwest surface winds and low wind speed in both seasons
169 (Supplementary Materials: Figure S6: a and S6: c). The high $PM_{2.5}$ loadings associated with
170 low wind speed indicate the significant contribution of near sources. While the landfill is
171 located at west of the sampling site, high $PM_{2.5}$ levels were potentially due to the influence of
172 local activities that transferred from the landfill. However, more than 50% of surface winds
173 were from the south or north in winter and south in summer from which low to high levels of
174 $PM_{2.5}$ were also observed under these conditions. The dominant wind directions at SENT was
175 east in winter and summer. The $PM_{2.5}$ loadings were observed to increase when surface winds

176 were from the east (from landfill) and northwest (where the downtown area is around 4 km
177 away from SENT) in winter (Supplementary Materials: Figure S6: b), which is consistent with
178 the prevailing wind in winter in Hong Kong (Yim et al., 2009; Yim et al., 2010). The $PM_{2.5}$
179 levels at this site could possibly be due to local and regional PM sources in winter (Hou et al.,
180 2018; Luo et al., 2018; Tong et al., 2018; Yim et al., 2019). In summer, no significant hotspots
181 were identified after the analysis. The emission maps of respirable suspended particulate
182 (RSP), nitrogen oxides and sulfur dioxide can be referred to Figure S7-9 (Supplementary
183 Material).

184 Under real-time $PM_{2.5}$ monitoring, high $PM_{2.5}$ levels were observed in winter. The higher
185 average $PM_{2.5}$ concentrations coupled with prevalent northerly to northeasterly winds were also
186 observed during winter. This observation points to possibly a transfer of aged and contaminated
187 air masses from the Pearl River Delta region to Hong Kong. The lower average $PM_{2.5}$
188 concentrations during the summer could be due to prevailing southerly or southeasterly winds
189 drawing clean marine air masses from the South China Sea or the Northwest Pacific Ocean,
190 diluting $PM_{2.5}$ concentrations (Wang et al., 2005; Yuan et al., 2006). In addition, heavy rainfall
191 caused by the summer monsoon could remove ground-level $PM_{2.5}$ by wet deposition
192 (Supplementary Materials: Table S1). During daytime under wind directions predominantly
193 from landfills high $PM_{2.5}$ levels were observed, which suggested the $PM_{2.5}$ level could be
194 affected by anthropogenic activities (locomotion, waste process, landfill surface dust, soot and
195 mineral particles and vehicular exhaust) from the landfills.

196 A temporal pattern could be related to local meteorological factors. The local sea breeze was
197 dominant (lower $PM_{2.5}$ concentration) from midnight until the early morning, while land
198 breezes (higher $PM_{2.5}$ concentration) dominated in the remainder of the day. However, over
199 50% and 30% of surface winds were not from WENT and SENT landfills, respectively, and no
200 significant association was observed between wind frequency from landfills and integrated

201 PM_{2.5} mass concentrations. This implies PM_{2.5} loading from other wind directions was an
202 important contributing factor.

203

204 3.2 Particle morphology analysis

205 The airborne particles were classified into 3 types (soot aggregations, mineral matter and “other
206 types”) based on morphology and elemental compositions (Figure 4). Soot aggregates were
207 commonly seen in the samples. For example several small soot particles were observed
208 adhering to the surface of a non-crystalline (conchoidal fracture) glass particle (Figure 4: a-1).
209 These composite particles contained C, O, Na, Al, Si and K element and the atomic percentages
210 were 60.28%, 32.57%, 1.37%, 0.41%, 4.78%, and 0.58%, respectively. Other particles are seen
211 as agglomerations of small spheres that predominantly consist of soot (Figure 4: a-2). The
212 atomic percentages of C, O, Na, Al, Si, and K were 69.81%, 21.99%, 0.90%, 0.56%, 6.00%,
213 and 0.74%, respectively. Numerous studies have confirmed that these soot aggregates possess
214 the typical morphology of emissions from gasoline or diesel engines (Berube et al., 1999).
215 These soot aggregate particles were collected near the landfill sites, which supports the view
216 that gasoline/diesel combustion pollution (due to landfill activities) are a major component of
217 landfill particulate pollution.

218 The identified mineral particles were derived from sources such as soil (used to cover the waste
219 cells), resuspension of dust from unmade roadways, and other anthropogenic site activities (e.g.
220 construction dust) (Yue et al., 2006). Mineral particles typically had irregular shapes with
221 obvious crystalline structures rarely seen (Figure 4: b-1). The particles commonly consisted of
222 an aggregation of mineral and soot particles. Some mineral grains were shown to possess a
223 ‘platy’ morphology, an indication for clay minerals. The initial clay identification was further

224 supported by the presence of Mg, Al, Si, K and Fe elements (atomic percentages of Mg, Al, Si,
225 K and Fe were 0.36%, 1.67%, 10.13%, 1.24%, and 0.18%, respectively).

226 The origins of the particles in the ‘other’ category could not be confidentially identified from
227 their morphology or elemental compositions; a common problem in some industry-sourced
228 PM. Two examples are shown to illustrate the challenges presented when trying to identify the
229 particle origins using analytical electron microscopy. These are the irregular shapes (Figure 4:
230 c) and agglomerates type particles (Figure 4: d). The SEM-EDX analysis (Figure 4: c) revealed
231 a large Fe component (atomic percentage = 5.74%), and the particle was interpreted as iron
232 oxide (rust). The particles surrounding the Fe particles were predominately soot and platy
233 (probably clay) mineral particles. The analysis (Figure 4: d) was shown to have high Si
234 component (atomic percentage = 10.83%) with no visual indication of crystallinity, precluding
235 common Si minerals. A number of micron to sub-micron size ‘glass’ particles agglomerated
236 into a single particle is observed in the image. It is speculated that this could be a fragment of
237 sintered glass where the smaller particles formed as an agglomerate under fusing temperature.

238

239 3.3 Ambient concentrations of chemical components in sampling locations

240 The samples collected by Teflon filters were used for mass concentration analysis. In winter,
241 the highest average concentration of PM_{2.5} was observed in WENT, whereas the SENT shows
242 comparable PM_{2.5} concentration range to the TKO site (Supplementary Materials: Table S3).
243 Significant spatial variability of PM_{2.5} levels were observed in WENT and TSW only in winter
244 ($p < 0.05$). Significant differences between seasons were observed in WENT, SENT, TKO and
245 HT sites ($p < 0.05$). Lower concentrations in summer could be due to enhanced thermal
246 convection in the summer season, which is influenced by the Asian monsoon. The

247 southwesterly summer monsoon could transfer clean oceanic aerosols from oceans (South
248 China Sea and tropical Pacific Ocean) (Cao et al., 2004; Ho et al., 2003).

249 The OC and EC concentrations are shown in Table S4 (Supplementary Materials). Daily
250 variation of OC and EC were observed at WENT and TSW, in addition to SENT and TKO all
251 demonstrate similar trends (Supplementary Materials: Figure S11-12) and significant
252 correlations between these two sites were observed in both seasons ($p < 0.05$). In contrast,
253 significant spatial variability of OC and EC concentrations were only observed in WENT and
254 TSW in winter ($p < 0.05$). The average concentrations of OC show significant differences
255 between seasons in all sites ($p = 0.05$), whereas seasonal variability for EC was only observed
256 in WENT and HT. The seasonal variations of OC could be due to prevailing north/northeast
257 winds during winter that could transfer polluted/aged air masses from China. This condition
258 could couple with stable atmospheric conditions in winter and resulted in the higher OC
259 concentrations. The compositions of OC and EC in the PM_{2.5} at all locations in winter are in a
260 range of 17.2-29.1 and 4.4-5.0%, respectively. The contributions are lower in summer (3.9-
261 15.0 and 2.2-8.8% for OC and EC, respectively). However, high OC-EC correlations ($r^2 > 0.75$)
262 at all sampling sites in both seasons imply strong association between these two fractions and
263 similar sources emissions.

264 The average concentrations of water-soluble inorganic ions are summarized in Table S5
265 (Supplementary Materials). The NO₃⁻, SO₄²⁻ and NH₄⁺ are the three most abundant ions in this
266 study. The concentrations of these components further show statistically significantly different
267 between seasons in all sampling locations, except for SO₄²⁻ in TSW ($p = 0.05$). Sulphate was
268 the one of the major components in PM_{2.5} which contributed in a range of 6.6-42.3 % in PM_{2.5}
269 mass in winter. The contributions were higher at all sampling locations in summer (22.9-60.8
270 %). The NO₃⁻ and NH₄⁺ are also major constituents of atmospheric aerosols in Hong Kong with
271 noticeable seasonal variations. Lower temperatures and less precipitation during winter

272 favoured particulate NH_4NO_3 over HNO_3 , and therefore higher NH_4NO_3 concentrations were
273 observed in winter. Significant spatial variability of NO_3^- , SO_4^{2-} and NH_4^+ concentrations were
274 observed in WENT and TSW only in winter ($p = 0.05$). High Na^+ concentrations observed in
275 the stations could possibly be due to higher and persistent on-shore winds which generated
276 abundant sea water droplets and marine aerosols. The higher Na^+ concentration in summer than
277 winter could be potentially due to prevailing southerly or south-easterly winds in summer
278 drawing marine air masses with large amount of sea salts bearing ions from the South China
279 Sea or the Northwest Pacific Ocean.

280 The concentrations of elements are shown in Table S6 (Supplementary Materials). The average
281 concentrations of total elements accounted for a range of 3.2-6.3% of $\text{PM}_{2.5}$ mass in winter;
282 whereas in a range of 3.2-4.3% in summer. The average concentrations of total elements were
283 minimum in summer and maximum in winter at all sampling locations, and a number of
284 elements show significant differences between seasons, especially for crustal species ($p =$
285 0.05). However, vanadium (V), as a marker for oil combustion, shows distinct maximum in
286 summer and minimum in winter in all locations. Residual oils are commonly used in diesel/ship
287 engines which can produce significant amount of V emissions. Air flow over the ocean in
288 summer could possibly explain the elevated V concentration from ship emissions in summer.
289 Iron (Fe) is one of the major crustal elements in this study and the main source is from mineral
290 dust. The average concentrations of Fe in HT (winter: 288.4 ng m^{-3} ; summer: 83.8 ng m^{-3}) are
291 lower than the other four sampling sites (winter: $432.2\text{-}582.8 \text{ ng m}^{-3}$; summer: $123.3\text{-}165.0 \text{ ng}$
292 m^{-3}) in both seasons, this could possibly be due to the landfill and urban sampling sites having
293 stronger influences by the mineral/road dust than background site (HT). The HT sampling
294 station is in a remote area and far removed from any anthropogenic activities, $\sim 2.5 \text{ km}$ away
295 from major traffic (Shek O Road). The observed concentrations suggest potential influences

296 by the crustal matter in the four sampling stations, and the sites are considered to be in
297 proximity to the local urban sources.

298 The concentrations of PAHs are shown in Table S7 (Supplementary Materials). The total PAHs
299 concentration accounted for a range of 0.02-0.54% and 0.02-2.62 % in composition to the OC
300 concentration in winter and summer, respectively. Statistically significant differences between
301 seasons were observed in all sites ($p = 0.05$). The FLT, PHE, PYR, CHR and BbF were
302 dominant components in all sampling locations which contributed $\geq 50\%$ of the total PAHs.
303 The United States Environmental Protection Agency (U.S. EPA) priority PAHs (Group B2
304 PAHs) in this study are in similar concentrations range to the Hong Kong roadside area, but
305 lower than the concentrations in Guangzhou, Beijing and Xi'an (Leung et al., 2014; Zhang et
306 al., 2016; Xu et al., 2016). According to the Chinese National Standard GB3095-2012, the
307 maximum allowable 24 h average concentration for BaP is 2.5 ng m^{-3} (Zhang et al., 2016). The
308 concentrations of BaP at all locations were below the threshold limit. The diagnostic ratios for
309 PAHs were also determined and listed with other studies (Supplementary Materials: Figure
310 S13). The ratios of INP/INP + BghiP and FLT/FLT + PYR from five sampling locations were
311 in the range of 0.37-0.60 and 0.23-0.80, respectively. These ratios were consistent with a
312 previous study and further suggested potential mixed influences from wood, coal and petroleum
313 combustion (Okuda et al., 2010; Xu et al., 2016).

314

315 3.4 Oxidative potential - plasmid scission assay (PSA)

316 A positive dose-response relationship was identified between the amounts of DNA damage and
317 sample concentrations, which indicates that higher mass concentrations of PM could cause
318 higher oxidative potential. The TD_{50} and DNA damage (%) ($100 \mu\text{g ml}^{-1}$ dosage) are listed in
319 Table 1. The amount of damage to the plasmid DNA induced by $PM_{2.5}$ varied over the range

320 of 24-92 % and 27-96 % in winter and summer, respectively. The WENT (and TSW) show the
321 lowest average DNA damage (under $100 \mu\text{g ml}^{-1}$) in winter. The oxidative potential of $\text{PM}_{2.5}$
322 samples in TKO was higher than other locations in winter. In contrast, both WENT and SENT
323 show comparable DNA damage in summer. No samples demonstrated $> 80\%$ average DNA
324 damage in TKO. This suggests samples collected near landfill in summer could contain higher
325 oxidative capacity than in other locations. The DNA damage in summer was higher than winter
326 in all locations (except TKO) and significant differences between seasons were observed in
327 WENT, SENT, TSW and HT ($p < 0.05$). The results are consistent with a recent study in
328 Beijing (Shao et al., 2017). Variation of DNA damage at WENT and TSW, together with SENT
329 and TKO all showed significant correlations ($p < 0.05$) in summer.

330

331 3.5 Correlation analysis

332 3.5.1 Correlation between major chemical components

333 Correlation analysis was performed to identify associations between species. The influences of
334 water-soluble inorganic ions and carbonaceous aerosol to $\text{PM}_{2.5}$ mass were confirmed by high
335 correlations of $\text{PM}_{2.5}$ with OC, EC, ammonium, sulphate, and nitrate ($r > 0.7$, $p < 0.01$).
336 Sulphates and nitrates are major inorganic ions and were well correlated with ammonium in all
337 sites ($r > 0.5$, $p < 0.05$). The strong correlation between NH_4^+ and SO_4^{2-} , together with NH_4^+
338 and NO_3^- suggest that these ions primarily existed as ammonium sulphate ($(\text{NH}_4)_2\text{SO}_4$),
339 ammonium bisulphate (NH_4HSO_4) and ammonium nitrate (NH_4NO_3) state.

340 Total PAHs was in good correlations with OC, EC and K^+ ($r > 0.5$, $p < 0.05$) and the highest
341 correlation was observed between total PAHs with OC/nss-K^+ in WENT and SENT ($r > 0.7$, p
342 < 0.01) in winter. Non-sea-salt potassium (nss-K^+) was used to exclude the influence of

343 potassium derived from sea-salt and commonly used as source tracer for biomass burning
344 activities. The results indicated regional impact from continental China was a determinant
345 factor in winter. However, no significant association was observed between total PAHs and
346 nss-K⁺ in summer. Good correlations were observed between total PAHs and OC/EC, which
347 indicated local combustion source (e.g. vehicular emission) was one of major sources for PAHs
348 in summer. High Na⁺ concentrations could be potentially due to sea water droplets and marine
349 sources. The analysis showed Cl⁻ ions were correlated with Na⁺ ions only in HT and SENT (r
350 > 0.5 , $p < 0.05$). Both locations are in proximity to sea with rich sea-salt particles. Nevertheless,
351 reaction of nitric acid with sea-salt particles (NaCl) could generate sodium nitrate in the loss
352 of chloride as product of gaseous hydrochloric acid (Zhuang et al., 1999).

353

354 3.5.2 The relationship between pollutants and wind patterns

355 Wind direction is one of important factors to determine origin of air mass. The frequencies of
356 wind blowing from landfills (%) were calculated based on individual sampling days and the
357 results are shown in Table 2. High percentages of wind flow from landfills were observed in
358 summer at both locations ($p < 0.05$). Spatial variability was also observed, with high frequency
359 of wind flow from landfill at SENT in both seasons. The associations of wind flow from
360 landfills (%) with chemical components are shown in Table S8 (Supplementary Materials)
361 (only significant positive correlations were listed). Significant correlations ($p < 0.01$) were
362 observed between wind frequency from landfills with V (except SENT in summer), Cu and Cl⁻
363 ion (except in summer). In addition, NO₃⁻, Na⁺ and K⁺ showed fair correlations with wind
364 frequency. The results indicated significant concentrations of V, Cu, Cl⁻, NO₃⁻, Na⁺ and K⁺
365 were observed when the wind flow from landfill sites. However, no significant associations
366 were observed between DNA damage with wind frequency from landfills.

367

368 3.5.3 Correlation between chemical components and DNA damage

369 The results can be referred to Table 3 for information. Significant positive associations ($p <$
370 0.05) between chemical components and DNA damage were mainly observed in summer
371 (except Mn, Cd, EC and total PAHs in SENT; Na^+ in WENT; and Sb and Ba in HT during
372 winter). Good correlations were observed for oxidative potential against Zn, Cd, Pb, NH_4^+ , K^+
373 and total PAHs in SENT in summer. DNA damage was positively correlated with NH_4^+ and
374 K^+ in TSW; Pb and NH_4^+ in TKO; and with Zn and Cd in HT. These results are consistent with
375 Shao et al. (2017) that trace elements were associated with particle induced oxidative potential
376 in summer (Shao et al., 2017). However, poor correlations were observed between DNA
377 damage with V, Cu, Cl^- , NO_3^- , and Na^+ in WENT and SENT, which are the species with high
378 correlations to wind frequency flow from landfill sites. The results suggest that these potential
379 landfills orientated species are not associated with oxidative potential responses. In addition,
380 the PLS regression showed no statistically significant differences between physical/chemical
381 characteristics and bioreactivity responses.

382

383 3.5.4 Implication of the correlation analysis

384 The analysis shows significant correlations were observed between wind frequency from
385 landfills with V (except SENT in summer) and Cu (except in summer). Vanadium is a marker
386 for residual oil, exhausts from container ships/landfill machineries (e.g. high emissions from
387 site machineries due to poor maintenance or overloading) that potentially were the sources for
388 these pollutants. Copper (Cu) was identified as a noticeable element in WENT landfill, due to
389 significant amounts of Cu under wind blow from landfill. Both landfills are close to the

390 seashore, high Na⁺ and Cl⁻ concentrations could be potentially due to sea water droplets and
391 marine aerosols. Thus, the high association between Na⁺ and Cl⁻ with wind frequency from
392 landfills was observed in the analysis. However, no significant associations were observed
393 between DNA damage/TD₅₀ when increased wind frequency from landfills. In addition, no
394 association were observed between DNA damage with V and Cu, this implied the dominant
395 factor determining the DNA damage was potentially due to other local or regional sources,
396 rather than from a landfill site; although further studies will be necessary in the future (Duffin
397 and Berube, 2006). Significant associations ($p < 0.05$) were mainly observed between DNA
398 damage and heavy metals (Cd and Pb)/PAHs in summer (Liu et al., 2009; Adamson et al.,
399 2000; Xia et al., 2004). Moreover, the DNA damage induced by PM_{2.5} was notably higher in
400 summer than winter. In all of the anthropogenically–derived metals, Cd and Pb are recognized
401 as emitted by high temperature coal and oil combustion processes, such as landfill processing
402 facility (Uberoi et al. and Shadman, 1991). Past studies showed metals are responsible for the
403 generation of ROS, our findings are consistent with previous studies.

404 This study showed high PM_{2.5} levels during daytime under predominantly wind direction from
405 landfills. Significant associations were observed between DNA damage and heavy
406 metals/PAHs in summer. Emissions from machineries were one of the potential sources in
407 proximity of the landfills. No significant associations were observed between DNA damage
408 when increased wind frequency from landfills which indicated that PM_{2.5} loading from other
409 sources (e.g. regional sources) was an important contributing factor for DNA damage.
410 However, limitations occurred such as the sampling frequency was only in every three days for
411 a period of ~ 4 months in the two seasons and insufficient information about the landfills
412 processing facilities could hinder the evaluation of air pollutants levels.

413

414 **Acknowledgments**

415 This study was supported by the Research Grants Council of the Hong Kong Special
416 Administrative Region China (Project No. CUHK 412612).

417

418 **References**

419 Adamson, I., Prieditis, H., Hedgecock, C., Vincent, R., 2000. Zinc is the toxic factor in the lung response
420 to an atmospheric particulate sample. *Toxicol. Appl. Pharmacol.* 166, 111-119.

421

422 Berube, K. A., Jones, T. P., Williamson, B., Winters, C., Morgan, A. J., Richards, R., 1999.
423 Physicochemical characterisation of diesel exhaust particles: Factors for assessing biological
424 activity. *Atmos. Environ.* 33, 1599-1614.

425

426 Bitterle, E., Karg, E., Schroepel, A., Kreyling, W., Tippe, A., Ferron, G., Schmid, O., Heyder, J.,
427 Maier, K., Hofer, T., 2006. Dose-controlled exposure of A549 epithelial cells at the air-liquid
428 interface to airborne ultrafine carbonaceous particles. *Chemosphere* 65, 1784-1790.

429

430 Cao, J., Lee, S., Ho, K., Zou, S., Fung, K., Li, Y., Watson, J. G., Chow, J. C., 2004. Spatial and seasonal
431 variations of atmospheric organic carbon and elemental carbon in Pearl River Delta Region,
432 China. *Atmos. Environ.* 38, 4447-4456.

433

434 Charrier, J. G., McFall, A. S., Richards-Henderson, N. K., Anastasio, C., 2014. Hydrogen peroxide
435 formation in a surrogate lung fluid by transition metals and quinones present in particulate matter.
436 *Environ. Sci. Technol.* 48, 7010-7017.

437

438 Costa, D. L., Dreher, K. L., 1997. Bioavailable transition metals in particulate matter mediate
439 cardiopulmonary injury in healthy and compromised animal models. *Environ. Health Perspect.*
440 105, 1053.

441

442 Deed, C., 2004. Monitoring of particulate matter in ambient air around waste facilities, Technical
443 Guidance Document (Monitoring) M17, Publ, Environment Agency, Bristol, ISBN, 1, 322610.

444

445 Donaldson, K., Beswick, P. H., Gilmour, P. S., 1996. Free radical activity associated with the surface
446 of particles: a unifying factor in determining biological activity?. *Toxicol. Lett.* 88, 293-298.

447

448 Duffin, R., Berube, K., 2006. British Association for Lung Research-Summer 2005 Meeting Summary-
449 Abstracts. *Exp. Lung Res.* 32, 119-+.

450

451 Gilmour, P., Beswick, P., Donaldson, K., 1994. Effects of asbestos and a range of respirable industrial
452 fibres on super-coiled plasmid DNA. *Respiratory Med.* 88, 812-813.

453

454 HKEPD, 2015. *Monitoring of Solid Waste in Hong Kong, Waste Statistics for 2015*. The Government
455 of the Hong Kong Special Administrative Region, Hong Kong Environmental Protection
456 Department (HKEPD): (accessed 18.10.18).

457

458 HKEPD, 2016. *South East New Territories Landfill to receive only construction waste from January 6*;
459 The Government of the Hong Kong Special Administrative Region, Hong Kong Environmental
460 Protection Department (HKEPD): (accessed 18.10.18).

461

462 Ho, K., Lee, S., Chan, C. K., Jimmy, C. Y., Chow, J. C., Yao, X., 2003. Characterization of chemical
463 species in PM 2.5 and PM 10 aerosols in Hong Kong. *Atmos. Environ.* 37, 31-39.
464

465 Hou, X., Chan, C.K., Dong, G.H., Yim, S.H.L., 2018. Impacts of transboundary air pollution and local
466 emissions on PM2. 5 pollution in the Pearl River Delta region of China and the public health, and
467 the policy implications. *Environ. Res. Lett.* 14, 034005.
468

469 Jarup, L., Briggs, D., De Hoogh, C., Morris, S., Hurt, C., Lewin, A., Maitland, I., Richardson, S.,
470 Wakefield, J., Elliott, P., 2012. Cancer risks in populations living near landfill sites in Great
471 Britain. *Br. J. Cancer* 86, 1732.
472

473 Jones, T., Moreno, T., Bérubé, K., Richards, R., 2006. The physicochemical characterisation of
474 microscopic airborne particles in south Wales: a review of the locations and methodologies. *Sci.*
475 *Total Environ.* 360, 43-59.
476

477 Koshy, L., Paris, E., Ling, S., Jones, T., Bérubé, K., 2007. Bioreactivity of leachate from municipal
478 solid waste landfills—assessment of toxicity. *Sci. Total Environ.* 384, 171-181.
479

480 Koshy, L., Jones, T., Bérubé, K., 2009. Characterization and bioreactivity of respirable airborne
481 particles from a municipal landfill. *Biomarkers* 14, 49-53.
482

483 Leung, P., Wan, H., Billah, M., Cao, J., Ho, K., Wong, C. K., 2014. Chemical and biological
484 characterization of air particulate matter 2.5, collected from five cities in China. *Environ. Pollut.*
485 194, 188-195.
486

487 Lingard, J., Tomlin, A., Clarke, A., Healey, K., Hay, A., Wild, C., Routledge, M., 2005. A study of
488 trace metal concentration of urban airborne particulate matter and its role in free radical activity
489 as measured by plasmid strand break assay. *Atmos. Environ.* 39, 2377-2384.
490

491 Liu, J., Qu, W., Kadiiska, M. B., 2009. Role of oxidative stress in cadmium toxicity and carcinogenesis.
492 *Toxicol. Appl. Pharmacol.* 238, 209-214.
493

494 Luo, M., Hou, X., Gu, Y., Lau, N.-C., Yim, S.H.-L., 2018. Trans-boundary air pollution in a city under
495 various atmospheric conditions. *Sci. Total Environ.* 618, 132-141.
496

497 Macklin, Y., Kibble, A., Pollitt, F., 2011. Impact on health of emissions from landfill sites, Advice from
498 the Health Protection Agency.
499

500 Miller, M.R., Shaw, C.A., Langrish, J.P., 2012. From particles to patients: oxidative stress and the
501 cardiovascular effects of air pollution. *Future Cardiol.* 8, 577-602.
502

503 Moreno, T., Merolla, L., Gibbons, W., Greenwell, L., Jones, T., Richards, R., 2004. Variations in the
504 source, metal content and bioreactivity of technogenic aerosols: a case study from Port Talbot,
505 Wales, UK. *Sci. Total Environ.* 333, 59-73.
506

507 Okuda, T., Okamoto, K., Tanaka, S., Shen, Z., Han, Y., Huo, Z., 2010. Measurement and source
508 identification of polycyclic aromatic hydrocarbons (PAHs) in the aerosol in Xi'an, China, by
509 using automated column chromatography and applying positive matrix factorization (PMF). *Sci.*
510 *Total Environ.* 408, 1909-1914.
511

512 Palmer, S. R., Dunstan, F. D., Fielder, H., Fone, D. L., Higgs, G., Senior, M. L., 2005. Risk of congenital
513 anomalies after the opening of landfill sites. *Environ. Health Perspect.* 113, 1362.
514

515 Pope III, C. A., Thun, M. J., Namboodiri, M M., Dockery, D. W., Evans, J. S., Speizer, F. E., 1995.
516 Heath Jr, C. W. Particulate air pollution as a predictor of mortality in a prospective study of US
517 adults. *Am. J. Respiratory Critical Care Med.* 151, 669-674.
518

519 Rogge, W. F., Mazurek, M. A., Hildemann, L. M., Cass, G. R., Simoneit, B. R., 1993. Quantification
520 of urban organic aerosols at a molecular level: identification, abundance and seasonal variation.
521 *Atmos. Environ. Part A. General Topics* 27, 1309-1330.
522

523 Shao, L., Shen, R., Wang, J., Wang, Z., Tang, U., Yang, S., 2013. A toxicological study of inhalable
524 particulates by plasmid DNA assay: A case study from Macao. *Sci. China Earth Sciences* 56,
525 1037-1043.
526

527 Shao, L., Hu, Y., Shen, R., Schäfer, K., Wang, J., Wang, J., Schnelle-Kreis, J., Zimmermann, R.,
528 BéruBé, K., Suppan, P., 2017. Seasonal variation of particle-induced oxidative potential of
529 airborne particulate matter in Beijing. *Sci. Total Environ.* 579, 1152-1160.
530

531 Sillanpää, M., Frey, A., Hillamo, R., Pennanen, A., Salonen, R., 2005. Organic, elemental and inorganic
532 carbon in particulate matter of six urban environments in Europe. *Atmos. Chem. Phys.* 5, 2869-
533 2879.
534

535 Stone, V., Shaw, J., Brown, D., MacNee, W., Faux, S., Donaldson, K., 1998. The role of oxidative stress
536 in the prolonged inhibitory effect of ultrafine carbon black on epithelial cell function. *Toxicol. In*
537 *Vitro* 12, 649-659.
538

539 Tong, C.H.M., Yim, S.H.L., Rothenberg, D., Wang, C., Lin, C.-Y., Chen, Y.D., Lau, N.C., 2018.
540 Assessing the impacts of seasonal and vertical atmospheric conditions on air quality over the
541 Pearl River Delta region. *Atmos. Environ.* 180, 69-78.
542

543 Uberoi, M., Shadman, F., 1991. High-temperature removal of cadmium compounds using solid
544 sorbents. *Environ. Sci. Technol.* 25, 1285-1289.
545

546 U.S. EPA, 2013. *Municipal Solid Waste in the United States*; EPA: Washington, DC, 2013. United
547 States Environmental Protection Agency (US EPA):
548 <https://archive.epa.gov/epawaste/nonhaz/municipal/web/html/>: (accessed 18.10.18).
549

550 Wang, G., Wang, H., Yu, Y., Gao, S., Feng, J., Gao, S., Wang, L., 2003. Chemical characterization of
551 water-soluble components of PM 10 and PM 2.5 atmospheric aerosols in five locations of
552 Nanjing, China. *Atmos. Environ.* 37, 2893-2902.
553

554 Wang, T., Guo, H., Blake, D., Kwok, Y., Simpson, I., Li, Y., 2005. Measurements of trace gases in the
555 inflow of South China Sea background air and outflow of regional pollution at Tai O, Southern
556 China. *J. Atmos. Chem.* 52, 295.
557

558 Xia, T., Korge, P., Weiss, J. N., Li, N., Venkatesen, M. I., Sioutas, C., Nel, A., 2004. Quinones and
559 aromatic chemical compounds in particulate matter induce mitochondrial dysfunction:
560 implications for ultrafine particle toxicity. *Environ. Health Perspect.* 112, 1347.
561

562 Xiao, Z., Shao, L., Zhang, N., Wang, J., Chuang, H.-C., Deng, Z., Wang, Z., BéruBé, K., 2014. A
563 toxicological study of inhalable particulates in an industrial region of Lanzhou City, northwestern
564 China: Results from plasmid scission assay. *Aeolian Res.* 14, 25-34.
565

566 Xu, H., Ho, S. S. H., Gao, M., Cao, J., Guinot, B., Ho, K. F., Long, X., Wang, J., Shen, Z., Liu, S.,
567 2016. Microscale spatial distribution and health assessment of PM 2.5-bound polycyclic aromatic
568 hydrocarbons (PAHs) at nine communities in Xi'an, China. *Environ. Pollut.* 218, 1065-1073.

569 Yim, S., Fung, J., Lau, A., 2009. Mesoscale simulation of year-to-year variation of wind power potential
570 over southern China. *Energies* 2, 340-361.
571

572 Yim, S., Hou, X., Guo, J., Yang, Y., 2019. Contribution of local emissions and transboundary air
573 pollution to air quality in Hong Kong during El Niño-Southern Oscillation and heatwaves. *Atmos.*
574 *Res.* 218, 50-58.
575

576 Yim, S.H., Fung, J.C., Lau, A.K., 2010. Use of high-resolution MM5/CALMET/CALPUFF system:
577 SO₂ apportionment to air quality in Hong Kong. *Atmos. Environ.* 44, 4850-4858.
578

579 Yuan, Z., Yu, J., Lau, A., Louie, P., Fung, J., 2006. Application of positive matrix factorization in
580 estimating aerosol secondary organic carbon in Hong Kong and its relationship with secondary
581 sulfate. *Atmos. Chem. Phys.* 6, 25-34.
582

583 Yue, W., Li, X., Liu, J., Li, Y., Yu, X., Deng, B., Wan, T., Zhang, G., Huang, Y., He, W., 2006.
584 Characterization of PM_{2.5} in the ambient air of Shanghai city by analyzing individual particles.
585 *Sci. Total Environ.* 368, 916-925.
586

587 Zhang, L., Chen, R., Lv, J., 2016. Spatial and Seasonal Variations of Polycyclic Aromatic Hydrocarbons
588 (PAHs) in Ambient Particulate Matter (PM₁₀). *Bull. Environ. Contam. Toxicol.* 96, 827-832.
589

590 Zhuang, H., Chan, C. K., Fang, M., Wexler, A. S., 1999. Formation of nitrate and non-sea-salt sulfate
591 on coarse particles. *Atmos. Environ.* 33, 4223-4233.
592
593
594
595
596

597 **List of Tables**

598 Table 1 The average DNA damage induced by PM_{2.5} collected from five sampling
599 locations in winter and summer.

600 Table 2 The average frequencies (%) of wind blowing from landfills in winter and
601 summer.

602 Table 3 Spearman's rank correlation coefficients (r) between DNA damage and PM_{2.5}
603 components.

604

605 **List of Figures and Figure Legends**

606 Figure 1 Locations of sampling sites

607 Figure 2 Hourly average PM_{2.5} concentration at WENT in a) winter and b) summer.

608 Figure 3 Hourly average of PM_{2.5} concentration at SENT in a) winter and b) summer.

609 Figure 4 Scanning electron microscope images reveal morphologies of PM_{2.5} samples

610 near the landfill sites.

611 Table 1 The average DNA damage induced by PM_{2.5} collected from five sampling locations in winter and summer.

Sampling location	Winter		Summer	
	TD ₅₀ * (µg ml ⁻¹)	DNA damage** (%)	TD ₅₀ (µg ml ⁻¹)	DNA damage (%)
WENT	227.5±294.0	39.1±16.3	41.8±16.1	70.2±23.2
SENT	118.6±82.8	46.0±20.3	48.0±26.4	67.2±24.9
TSW	95.5±48.8	39.1±21.7	51.3±22.3	60.7±25.5
TKO	61.3±39.7	62.1±19.1	54.5±14.1	48.6±11.4
HT	102.8±82.5	43.0±18.2	63.3± 69.0	64.4±25.4

612 *The toxic dosage of particulate matter causing DNA damage (TD₅₀) denotes the toxic dosage of PM_{2.5} causing 50% DNA damage.

613 **The amount of damage to the plasmid DNA induced by PM_{2.5} under 100 µg ml⁻¹ dosage.

614

615 Table 2 The average frequencies (%) of wind blowing from landfills in winter and summer.

Sampling location	Winter*		Summer	
	Mean	Range	Mean	Range
WENT	30.7±13.9	4.3-51.8	43.3±19.1	7.1-71.8
SENT	60.8±17.7	11.2-84.0	66.1±18.7	18.6-84.8

616 *The frequencies (%) were based on individual sampling days.

617

618

619

620

621

622

623 Table 3 Spearman's rank correlation coefficients (r) between DNA damage and PM_{2.5} components.
624

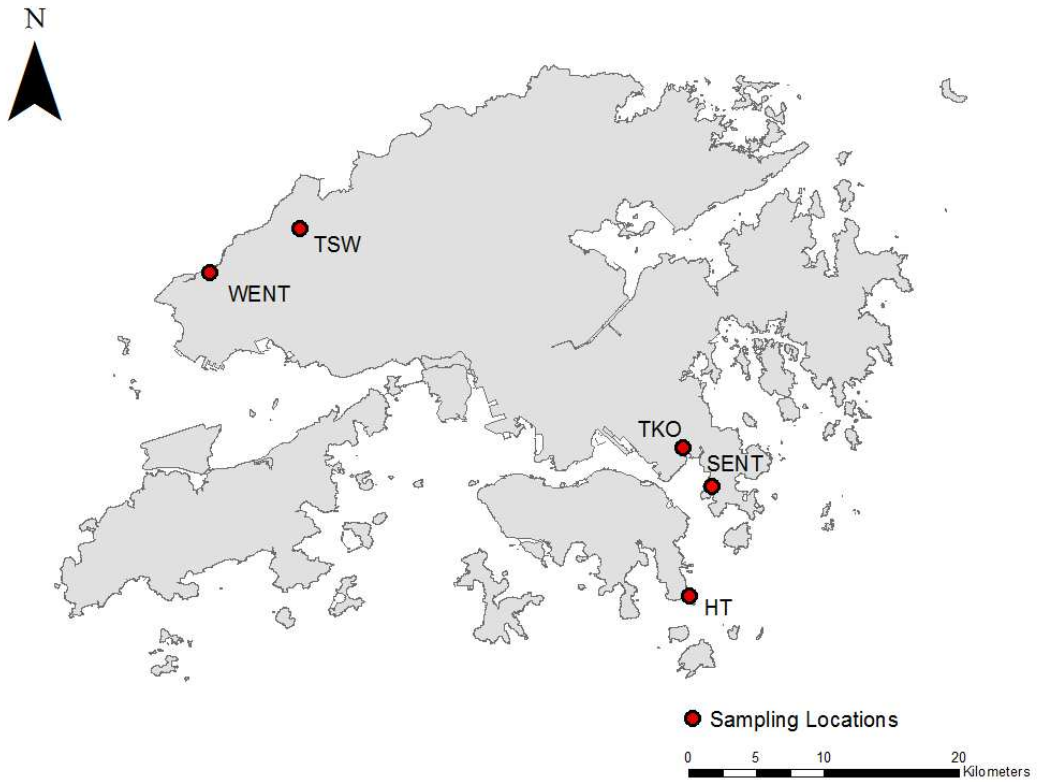
Components	WENT		SENT		TSW		TKO		HT	
	Winter	Summer	Winter	Summer	Winter	Summer	Winter	Summer	Winter	Summer
Mg	0.26	-0.16	-0.05	-0.61	-0.31	-0.32	-0.47	-0.84	-0.12	-0.68
Ca	-0.57	-0.39	0.25	-0.50	-0.15	-0.64	-0.77	-0.02	-0.02	-0.31
V	-0.06	-0.09	-0.05	-0.76	0.12	-0.27	-0.63	-0.49	-0.05	-0.30
Cr	-0.01	0.03	-0.32	-0.51	-0.42	-0.23	-0.62	-0.51	0.22	-0.53
Mn	0.08	0.21	0.62	0.05	0.17	0.09	-0.73	-0.21	-0.12	0.04
Fe	-0.14	0.19	-0.02	-0.70	0.63	-0.13	-0.13	-0.46	-0.17	-0.03
Ni	0.04	0.09	-0.55	-0.80	0.46	-0.40	-0.02	-0.47	-0.34	-0.41
Cu	0.01	0.01	-0.30	-0.58	-0.42	0.13	0.45	0.05	-0.01	-0.52
Zn	-0.10	0.34	-0.05	0.77⁺⁺	0.25	0.35	0.30	0.54	-0.05	0.72
As	0.07	0.44	0.47	0.24	0.44	0.45	0.07	0.39	0.00	0.24
Cd	-0.13	0.42	0.67⁺	0.82⁺⁺	-0.32	0.62	0.32	0.46	0.31	0.71⁺⁺
Sb	-0.04	-0.10	0.32	-0.01	-0.05	0.18	0.30	-0.22	0.67	-0.48
Ba	-0.29	-0.33	0.35	0.12	-0.76	-0.33	-0.07	-0.10	0.60	-0.10
Pb	-0.13	0.36	0.22	0.79⁺⁺	0.36	0.35	0.37	0.67⁺	0.13	0.46
OC	-0.53	0.52	0.23	0.56	-0.08	0.47	0.38	0.58	0.21	0.27
EC	-0.51	0.36	0.83⁺⁺	0.18	-0.14	0.34	0.48	0.36	-0.26	0.10
Cl ⁻	0.61	-0.41	-0.28	-0.80	-0.03	-0.59	0.40	-0.56	0.05	-0.72
NO ₃ ⁻	0.07	-0.48	-0.55	-0.51	0.05	-0.06	0.10	-0.30	0.20	-0.50
SO ₄ ²⁻	0.10	-0.26	0.10	-0.32	-0.03	-0.37	-0.55	-0.15	-0.08	-0.09
Na ⁺	0.62	-0.10	-0.35	-0.93	0.12	-0.37	-0.20	-0.80	0.09	-0.69
NH ₄ ⁺	0.22	0.16	-0.18	0.73⁺	-0.08	0.66⁺	-0.37	0.62⁺	-0.05	0.52
K ⁺	-0.05	-0.09	0.53	0.90⁺	0.58	0.90⁺	0.50	0.15	-0.25	0.43
ACE	0.13	-0.19	-0.80	-0.31	0.51	0.16	-0.10	-0.41	0.36	-0.35
FLU	0.05	0.42	-0.03	0.16	0.37	0.42	0.03	-0.05	0.46	-0.68
PHE	-0.78	0.27	0.62	-0.02	0.41	0.60	0.30	0.22	-0.26	-0.16
ANT	-0.85	0.24	0.47	-0.36	0.63	0.43	0.00	0.01	-0.24	-0.13
FLT	-0.72	0.31	0.65	0.89⁺⁺	-0.22	0.48	0.45	0.79⁺⁺	-0.28	0.52
PYR	-0.78	0.33	0.70⁺	0.85⁺⁺	0.19	0.77⁺⁺	0.32	0.76⁺⁺	-0.27	0.36
BaA	-0.34	0.41	0.50	0.67⁺	0.48	0.59	-0.12	0.80⁺⁺	-0.38	0.53
CHR	-0.34	0.18	0.70⁺	0.65⁺	0.31	0.59	0.15	0.79⁺⁺	-0.30	0.46
BbF	-0.56	0.23	0.67⁺	0.78⁺⁺	0.58	0.48	0.08	0.80⁺⁺	-0.33	0.49
BkF	-0.47	0.20	0.75⁺	0.71⁺	0.41	0.50	0.18	0.72⁺	-0.42	0.59⁺
BaF	-0.58	0.21	0.83⁺⁺	0.76⁺⁺	0.56	0.51	0.03	0.87⁺⁺	-0.33	0.44

BeP	-0.67	0.27	0.80⁺⁺	0.77⁺⁺	0.58	0.45	0.10	0.76⁺⁺	-0.35	0.53
BaP	-0.67	0.40	0.85⁺⁺	0.71⁺	0.32	0.50	0.15	0.72⁺	-0.20	0.48
PER	-0.58	0.44	0.60	0.56	0.53	0.43	-0.48	0.69⁺	-0.05	0.60⁺
INP	-0.67	0.29	0.85⁺⁺	0.69⁺	0.58	0.46	0.25	0.61⁺	-0.31	0.39
BghiP	-0.67	0.35	0.82⁺⁺	0.67⁺	0.58	0.42	-0.03	0.58	-0.17	0.41
DahA	-0.67	0.27	0.83⁺⁺	0.65⁺	0.46	0.43	0.21	0.49	-0.34	0.44
COR	-0.65	0.36	0.58	0.85⁺⁺	0.58	0.43	-0.28	0.70⁺	-0.02	0.25
Total PAHs	-0.67	0.29	0.72⁺	0.64⁺	0.58	0.45	0.03	0.78⁺⁺	-0.24	0.36

625 +, positive correlation, $p < 0.05$.

626 ++, positive correlation, $p < 0.01$.

627

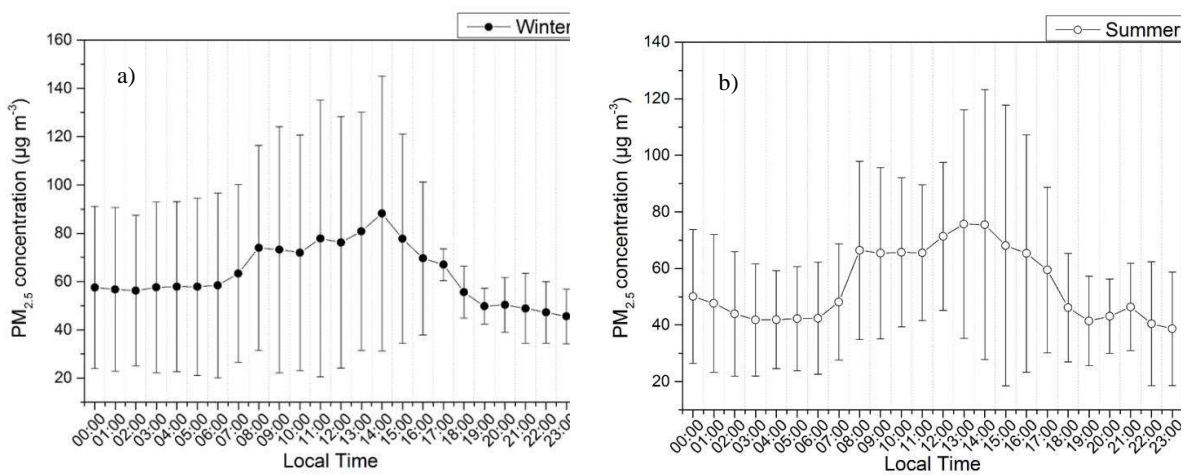


628

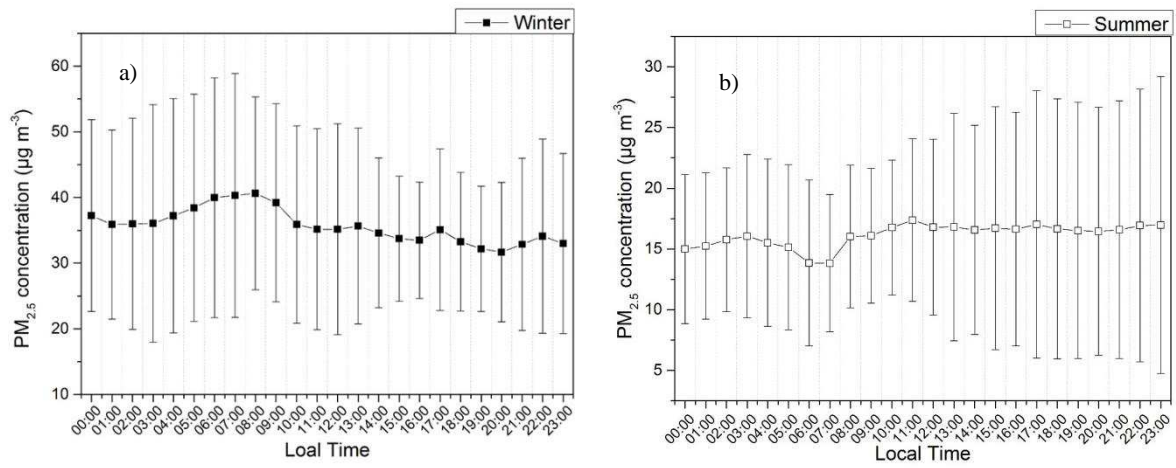
629 Figure 1 Locations of sampling sites.

630

631



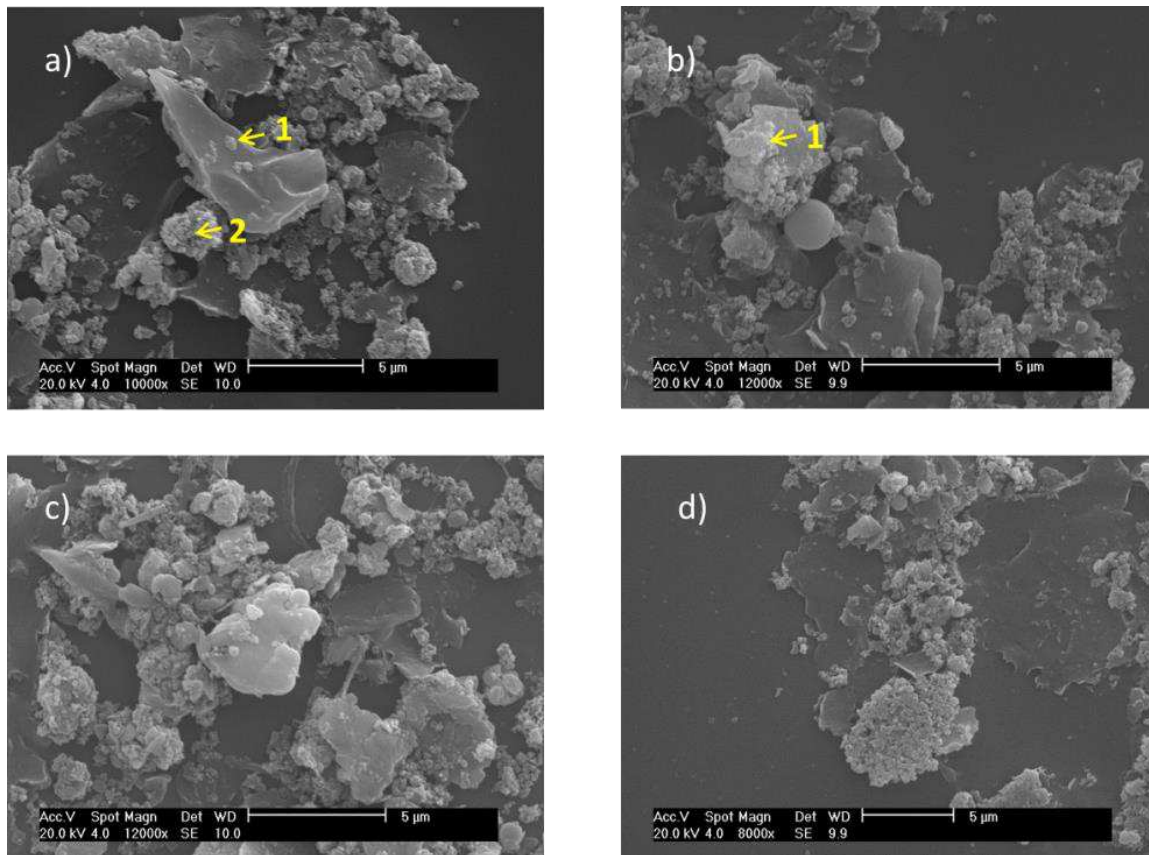
632 Figure 2 Hourly average PM_{2.5} concentration at WENT in a) winter and b) summer.



633 Figure 3 Hourly average of PM_{2.5} concentration at SENT in a) winter and b) summer.

634

635



636

637 Figure 4 Scanning electron microscope images reveal morphologies of PM_{2.5} samples

638

near the landfill sites.

639

640